A Sidelobe Level Minimization Mismatched Filter using Continuous Phase Frequency-Shift Keying Codes for the Off-Grid Delay Problem

Maria-Elisavet Chatzitheodoridi*, Abigael Taylor*, Olivier Rabaste*, Hélène Oriot*
* *DEMR, ONERA, Université Paris-Saclay*
F-91123 Palaiseau - France
Email: {maria-elisavet.chatzitheodoridi, abigael.taylor, olivier.rabaste, helene.oriot} @onera.fr

***Abstract*—Sidelobe suppression is an essential criterion for radar performance, especially for off-grid points of sampled signals. In this paper, a mismatched filter that minimizes the average sidelobe energy over a continuous time interval is proposed. The main contribution of this paper is the optimization of this problem for continuous phase modulated signals, which present relevant properties for a dual radar-communications system. It is shown that the optimization problem is convex, thus it provides an optimal solution. The performance of the proposed filter in terms of mean Integrated Sidelobe Level is then compared to the classical matched filter, as well as to the usual on-grid mismatched filter, through simulations. The obtained results show that the proposed filter presents greater performance over the continuous sampling cell than the others.**

***Index Terms*—Mismatched Filter, Optimal, Delay, Continuous Interval, off-Grid, Integrated Sidelobe Level, Continuous Phase Modulation, Waveform Diversity, RadComm System.**

I. Introduction

In radar applications, the most common pulse compression technique for target detection is the matched filter (MF) that aims at maximizing the target signal-to-noise ratio (SNR) by correlating the received signal with the transmitted one [1]. However, potentially strong sidelobes are created by the matched filter in the presence of strong targets, which may prevent the detection of weaker ones [2]. In such cases, sidelobe level control is necessary and can be achieved by replacing the matched filter by a different one, which for instance minimizes the sidelobe energy. Theses types of filters are denoted as mismatched filters, since the correlation is not performed with the transmitted signal [2]. Detailed literature exists on mismatched filter optimization using different minimization criteria and parameters [3]–[8].

Mismatched filters are widely used in radar applications. For example, for linear phase steering vectors and chirp signals, compression is usually performed using a weighting window [9], that provides lower sidelobes, at the price of a larger mainlobe. For sampled signals, mismatched filtering can be obtained as an optimal solution of a convex optimization problem. The choice of the cost function and the constraints of the optimization problem depends mainly on the specific radar application. Most papers define the cost function with respect either to the Peak-to-Sidelobe Ratio (PSLR) or the Integrated Sidelobe Level (ISL) [5]–[7], [10]–[12]. In the case of radar pulses, the resulting mismatched filter provides the optimal delay compression of the target response in terms of sidelobe level for the considered sampled signal. The signal sampling period naturally defines a grid that also samples the delay parameter space. However, the signal back-scattered by the target undergoes a delay shift that may not coincide with this sampling grid. In such a case, off-grid mismatch may occur [8], [13], which potentially degrades the sidelobe level. It is thus necessary to improve the mismatched filter optimization in order to tackle off-grid delay shifts by minimizing the sidelobe level energy over a continuous interval. In the paper [8], the off-grid problem over a continuous interval in case of steering vectors and chirp pulses is considered. In the article [14], a mismatched filter over a continuous Doppler interval using phase codes is provided.

In this paper, continuous phase frequency-shift keying (CPFSK) signals are considered. They belong to a continuous phase modulated (CPM) signal category [15]. Since the phase of such signals is continuous, as stated by their name, they present interesting characteristics regarding spectral containment, which make them a good candidate for dual radar-communication systems [16]. Hence for spectrum sharing applications, CPFSK are of particular interest. Unfortunately, their use induces potentially strong sidelobes, as well as off-grid mismatches due to continuous phase rotation between two consecutive delay samples. Thus, we introduce in this paper the problem of designing an optimum mismatched filter for CPFSK codes, that minimizes the average Integrated Sidelobe Level over a continuous delay shift interval, spanning the sampling cell. We calculate the associated cost function using these communication signals over the sampling cell and show that its optimization depends strongly on some signal characteristics, for example the embedded symbols. The proposed optimization problem is convex with linear and quadratic convex constraints so it can be efficiently solved using a convex solver such as *CVX* [17]. The obtained solution is an optimal filter robust over the sampling cell.

The performance in terms of ISL of the proposed mismatched filter is compared with the classical matched filter and the optimal on-grid mismatched filter, for randomly drawn CPFSK signals. As expected, the on-grid mismatched filter provides the best ISL for delays selected on the grid, but the proposed mismatched filter is more robust for off-grid delays and provides the best average ISL over the considered delay interval.

This paper is organized as follows. Section II provides mathematical formulations of the CPFSK signals and the mismatched filter definition. Section III is dedicated to the derivation of the proposed optimized filter over the continuous delay sampling cell using CPFSK. Finally, section IV presents on one side simulation framework and on the other side, filter performance and results comparison.

II. Problem Statement

A. Continuous Phase Frequency-Shift Keying (CPFSK) Signals

In communication applications, diverse coding schemes may be used to transmit desired information, some of which are well known such as Phase Shift Keying and Quadrature Amplitude Modulations [18]. In these two strategies, communication symbols are selected from a discrete set of values in the complex plane. Direct encoding of these symbols without specific phase shaping usually leads to brutal phase changes when transitioning from one symbol to the following one. These brutal transitions tend to increase the out-of-band energy. On the contrary, continuous phase modulated (CPM) signals ensure the phase transition continuity from one symbol to another, which prevents spectrum spreading outside of the band.

For the CPM codes, the embedded symbols $\mathbf{I} = [I_1, I_2, \ldots]$ belong to the set $\{\pm 1, \pm 3, ..., \pm(M-1)\}$ also called M-ary alphabet, with M the number of different possible symbols in the constellation. The constellation determines the number k of bits per symbol through the expression $2^k = M$. The phase of a CPM signal is generally expressed as [15]:

$$\begin{aligned}\phi(t;\mathbf{I}) &= 2\pi \sum_{i \le n} I_i h_i \int_0^t g(\tau - iT) d\tau \\ &= 2\pi \sum_{i \le n} I_i h_i u(t - iT), \qquad nT < t \le (n+1)T\end{aligned}$$

where t is the time variable, h_i is the modulation index in $]0,1[$ for the i^{th} sample, I_i is the i^{th} information symbol, T is the time chip duration and $u(t)$ is a phase smoothing response function,

$$u(t) = \int_0^t g(\tau) d\tau.$$

In this paper, a special category of CPM is considered, called continuous-phase frequency-shift keying (CPFSK) [15]. It takes into consideration a constant modulation index h, such that $h = h_i, \forall i$ and a rectangular smoothing function g.
By extension the function u is equal to 0 for $t < 0$, equal to $\frac{t}{2T}$ when $t \in [0, T[$ and equal to 0.5 for $t \ge T$.

Finally, the CPFSK signal can be formulated as $s(t;\mathbf{I}) = e^{j\phi(t;\mathbf{I})}$, with the phase ϕ expressed as [15],

$$\phi(t;\mathbf{I}) = \pi h \sum_{i<n} I_i + \frac{\pi h}{T}(t - nT) I_n, \qquad nT < t \le (n+1)T. \tag{1}$$

B. Delayed CPFSK Signal and Mismatched Filter Output

In the literature, the mismatched filter is mostly expressed for sampled signals [3], [7]. The particular case of chirp signals is considered in [8]. In this section, mathematical expressions of the delayed received signal and the corresponding mismatched filter output are derived.

Let $\mathbf{s}$ be the N-length sampled signal obtained by sampling the continuous CPFSK waveform,

$$\mathbf{s} = \begin{bmatrix} s_1 & s_2 & \ldots & s_N \end{bmatrix}^T,$$

where $.^T$ is the transpose operator.
The signal back-scattered by the target returns to the antenna with a given delay τ. The i^{th} component of the noiseless delayed received signal $\mathbf{r}^\tau$ can then be expressed as:

$$r_i^\tau = s(t_i - \tau) = s_i \exp\left(-\frac{j\pi h}{T} I_{n_i} \tau\right), \quad \forall i \in [\![1, N]\!], \tag{2}$$

where t_i is the i^{th} time sample which depends on the sampling period T_s, T is the chip duration such that $T = \alpha T_s$ with $\alpha \in [1, +\infty[$ and n_i is the symbol index associated to the i^{th} time sample. The undergoing delay shift τ lies in $\left[-\frac{T_s}{2}, \frac{T_s}{2}\right]$.

At reception, the delayed signal is compressed using a mismatched filter in order to perform target detection while respecting a low sidelobe energy performance. The length K of the mismatched filter $\mathbf{q} \in \mathbb{C}^K$ can be equal to or greater than the length of the signal ($K \ge N$).
The noiseless output signal can be expressed as

$$\mathbf{y}(\tau) = \mathbf{\Lambda}^*(\tau)\mathbf{q}, \tag{3}$$

where $.^*$ is the complex conjugate,

$$\mathbf{q} = \begin{bmatrix} q_1 & q_2 & \ldots & q_K \end{bmatrix}^T,$$

and where $\mathbf{\Lambda}(\tau)$ is the correlation matrix of size $(K+N-1) \times K$ of the delayed signal $\mathbf{r}^\tau$, defined by

$$\mathbf{\Lambda}(\tau) = \begin{bmatrix} r_N^\tau & 0 & \ldots & \ldots & 0 \\ \vdots & \ddots & \ddots & & \vdots \\ r_1^\tau & \ddots & r_N^\tau & \ddots & \vdots \\ 0 & \ddots & \vdots & \ddots & 0 \\ \vdots & \ddots & r_1^\tau & \ddots & r_N^\tau \\ \vdots & & \ddots & \ddots & \vdots \\ 0 & \ldots & \ldots & 0 & r_1^\tau \end{bmatrix}.$$

If the filter is chosen as $\mathbf{q} = \mathbf{s}$, then the classical matched filter is obtained. However, the delayed signal $\mathbf{r}^\tau$ differs from the sampled signal $\mathbf{s}$ as shown by the equation (2), thus inducing a mismatch between the signal used for comparison and the received signal. We will refer to this mismatch as the off-grid problem.

III. Optimization Problem Formulation using the ISL criterion for the off-grid delay problem

When referring to the Integrated Sidelobe Level for the mismatched formulation, extensive literature is available [5]–[7], [10]–[12]. Yet, the off-grid problem is generally not considered except for the chirp pulse case in [8], [19]. In this paper, the off-grid problem is taken into account, by searching for the mismatched filter that minimizes the average sidelobe level produced by CPFSK signals over all possible delay shifts in a sampling cell. The cost function minimization problem is defined using the L_2-norm in order to consider the Integrated Sidelobe Level (ISL). It is defined as the energy of all sidelobes [20], and by considering the sampled signal, it is expressed as,

$$ISL\,(\mathbf{y}) = 10\ \log_{10} \sum_{k \in \Omega_{SL}} |y_k|^2, \tag{4}$$

where Ω_{SL} is the sidelobe sample set.

The delay shift variable τ is selected to be uniformly distributed over a sampling period T_s. The defined interval, where τ is optimized, corresponds to a sampling interval,

$$\Theta = \left(-\frac{T_s}{2}, \frac{T_s}{2}\right). \tag{5}$$

In other words, the middle of each interval is the on-grid sample while any other value in Θ corresponds to an off-grid delay. Two different delay shifts from the interval Θ will lead to two different sampled signals $\mathbf{r}^\tau$ and thus the outputs are not going to be identical, which may result to highly unlike sidelobe levels. The minimization problem is thus expressed as [8], [14]:

$$\begin{aligned} \min_{\mathbf{q}} \quad & \mathbb{E}_\tau\big(||\mathbf{F}\mathbf{y}(\tau)||_2^2\big), \\ \text{s.t.} \quad & \mathbf{s}^H\mathbf{q} = \mathbf{s}^H\mathbf{s}, \\ & \mathbf{q}^H\mathbf{q} \leq 10^{\frac{\beta}{10}}\mathbf{s}^H\mathbf{s}, \end{aligned} \tag{6}$$

where $\mathbf{F}$ is a diagonal matrix of ones except for some zero values which correspond to the mainlobe position indices and β is a positive constant in dB that expresses the maximum acceptable loss-in-processing gain [3].

As mentioned in [8], the first constraint allows to discard the trivial null solution and is convex because of its linearity and the second one enables to constraint the loss-in-processing gain and is also convex as it is a positive semi-definite quadratic constraint. Globally, since the L_2-norm is convex, the optimization problem is thus convex, with convex constraints. As a consequence, any local optimum of the optimization problem is necessarily a global optimum.

Knowing the delay shift is uniformly distributed over the interval Θ, the cost function expectation is calculated as:

$$\begin{aligned} \mathbb{E}_\tau\big(||\mathbf{F}\mathbf{y}(\tau)||_2^2\big) &= \frac{1}{T_s}\int_\Theta ||\mathbf{F}\mathbf{y}(\tau)||_2^2 d\tau \\ &= \frac{1}{T_s}\mathbf{q}^H\left[\int_\Theta \mathbf{\Lambda}^T(\tau)\mathbf{F}\mathbf{\Lambda}^*(\tau)d\tau\right]\mathbf{q} \\ &= \frac{1}{T_s}\mathbf{q}^H\mathbf{M}_\Theta\mathbf{q} \\ &= \frac{1}{T_s}||\mathbf{M}_\Theta^{\frac{1}{2}}\mathbf{q}||_2^2, \end{aligned} \tag{7}$$

with $(M_\Theta)_{k,l} =$

$$\sum_{a=1}^{K+N-1} \Lambda_{k,a}^T(0)F_{a,a}\Lambda_{a,l}^*(0)T_s\ \text{sinc}\Big[\frac{h}{T}(I_{n(N+l-a)} - I_{n(N+k-a)})\frac{T_s}{2}\Big].$$

Thus, the cost function strongly depends on some signal characteristics such as the modulation index h, the chip duration T and the embedded symbols $\mathbf{I}$.

Proof. The components of the correlation matrix $\mathbf{\Lambda}(\tau)$ can be expressed as :

$$\Lambda_{k,l}(\tau) = \begin{cases} s(t_{N+l-k} - \tau), & |l-k| \leq N \\ 0, & \text{otherwise.} \end{cases}$$

Let $k, l \in [\![1, N]\!]$. The matrix $\mathbf{M}_\Theta$ elements can be expressed as

$$\begin{aligned} (M_\Theta)_{k,l} &= \int_\Theta \Big(\mathbf{\Lambda}^T(\tau)\mathbf{F}\mathbf{\Lambda}^*(\tau)\Big)_{k,l} d\tau \\ &= \int_\Theta \sum_{a=1}^{K+N-1} \Lambda_{a,k}(\tau)F_{a,a}\Lambda_{a,l}^*(\tau)d\tau \\ &= \int_\Theta \sum_{a=1}^{K+N-1} s(t_{N+k-a})\exp\left(-\frac{j\pi h}{T}I_{n(N+k-a)}\tau\right) \\ &\qquad F_{a,a}\ s^*(t_{N+l-a})\exp\left(\frac{j\pi h}{T}I_{n(N+l-a)}\tau\right)d\tau \\ &= \sum_{a=1}^{K+N-1} s(t_{N+k-a})\ F_{a,a}\ s^*(t_{N+l-a}) \\ &\qquad \int_{-\frac{T_s}{2}}^{\frac{T_s}{2}} \exp\left(\frac{j\pi h}{T}\left(I_{n(N+l-a)} - I_{n(N+k-a)}\right)\tau\right)d\tau \\ &= \sum_{a=1}^{K+N-1} \Lambda_{k,a}^T(0)F_{a,a}\Lambda_{a,l}^*(0)\ T_s \\ &\qquad \text{sinc}\left[\frac{h}{T}\left(I_{n(N+l-a)} - I_{n(N+k-a)}\right)\frac{T_s}{2}\right]. \end{aligned}$$

$\square$

IV. Simulation and Results

This section is dedicated to the simulation framework and the proposed filter performance. Table I lists some signal characteristics and simulation parameters used for the generation of Figure 1, as for the rest of the results some parameters become variables.

Parameters	**Value**
Bandwidth B	165.5 MHz
Pulse Duration T_p	1 μs
Modulation index h	0.5
Chip duration T	10 ns
Sampling Period T_s	5 ns
Constellation	4
Allowed loss in processing gain β	2 dB

Table I: Simulation Parameters for Figure 1.

A. Framework Specification and Notations

The continuous interval Θ is used, as defined in (5), and it depends on the CPFSK signal sampling period T_s. For the sake of simplicity, the on-grid point is considered to be in the middle of this interval and the time sampling is defined as $t_i = \frac{T_s}{2} + (i-1)T_s$, with $i \in [\![1, N]\!]$, in order to avoid undefined boundary points. At these time samples, the delay shift τ is applied, where $\tau \in \Theta$.

As mentioned, the mismatched filter formulation is a convex optimization problem whose optimal solution can be obtained using a convex solver. Here, the implementation is performed using the Matlab toolbox *CVX: Matlab Software for Disciplined Convex Programming* [17]. The allowed chosen maximum loss-in-processing gain in the simulations is $\beta = -2$dB.

Several filters mentioned in the literature are implemented for the sake of comparison. Firstly, the classical matched filter is considered and it is denoted by *'MF'*. The second one is denoted by *'MMF_0^K'* and it minimizes the sidelobe level energy only for one on-grid value, which corresponds to no delay shift, proposed for instance in [3]. Finally, the mismatched filter proposed in this paper is denoted by *'MMF_τ^K'*.

In the performance study, two different mismatched filter lengths K are considered, first of length N which is denoted with an exponent $\cdot^N$ and then of length $3N$, denoted by an exponent $\cdot^{3N}$.

B. Filter Performance

This subsection provides comparative results between the generated filters over the sampling cell and for different filter lengths.

Figure 1 illustrates the mean ISL obtained for the different filters, applied for 100 Monte Carlo simulations of CPFSK pulses with randomly drawn information symbols but with the same sampling frequency factor α over the given Θ, and the same symbol number. At the same time, Figure 1 provides the standard deviation presented for each delay shift. The need of computing the deviation from the mean values comes from the randomness of the information embedded in the CPFSK phase signal.

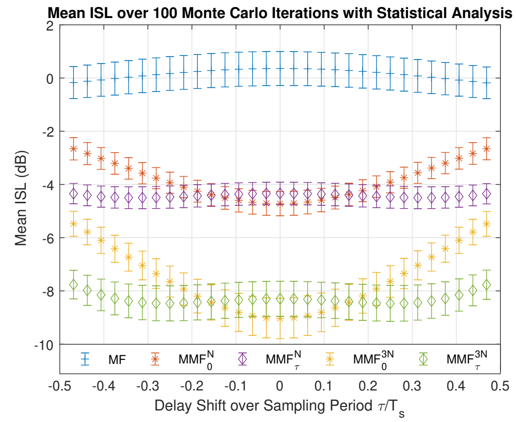

Figure 1: Mean ISL for CPFSK signals over the sampling cell Θ after 100 Monte Carlo iterations. The standard deviation is represented by the bars around the mean value of the ISL obtained on the Monte Carlo iterations. The chosen sampling rate is 2 sampling points per symbol and the symbol number is 100 per CPFSK signal.

As expected, for a chosen filter length K, the filter optimized for no delay shift MMF_0^K provides better sidelobe energy performance for zero delay shift and the neighborhood of zero up to $\frac{|\tau|}{T_s} \approx 0.15$. However for higher delay shifts, this filter is no longer optimal and the sidelobe energy increases. Contrariwise, the mismatched filter MMF_τ^K optimized over the continuous delay shift interval produces larger sidelobe levels near the zero delay shift than MMF_0^K, but lower ones at higher delay shifts, as shown in Figure 1. This behavior is coherent since our filter is optimized with respect to the average off-grid energy. In addition, the averaged ISL for the filter optimized on the whole considered delay interval is the best, as can be seen from Figure 2 and Figure 3, especially for low frequency rate. For the classical matched filter *MF*, the sidelobe level is quite higher compared to the mismatched filters.

The filter length plays a critical role in its performance. When using a longer filter, the computed sidelobe energy is decreased, at the price of a greater computational cost. For instance, the filters MMF_0^{3N} and MMF_τ^{3N}, of length $K = 3N$, provide a lower ISL than the filters MMF_0^N and MMF_τ^N, of length $K = N$, over the sampling cell, as indicated not only in Figure 1, but also in Figure 2 and Figure 3. Longer filters are not considered, as the combination of the ISL performance and the computational cost is not profitable compared to the $3N$-length filter.

Figure 2 provides the mean ISL of a 50-symbol random CPFSK signal for different sampling frequency factors α. 50 Monte Carlo iterations are considered here in order to provide generalized compression solutions of the mean ISL over the sampling cell, so thah mean and standard deviation values can be computed. When the sampling fre-

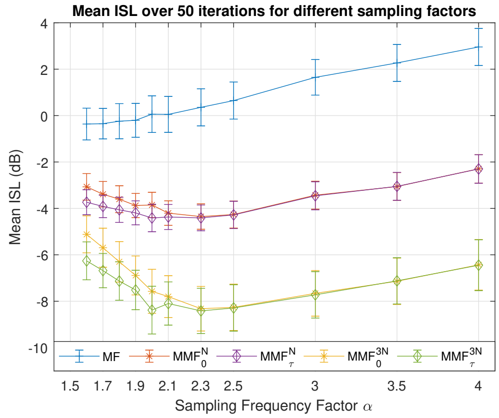

Figure 2: Mean and standard deviation values on 50 Monte Carlo iterations for the mean ISL of CPFSK signals over the sampling cell with respect to the sampling frequency factor α. Here, the CPFSK signals contain 50 symbols.

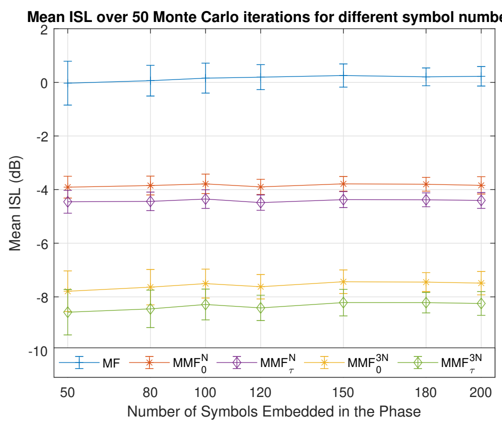

Figure 3: Mean and standard deviation values on 50 Monte Carlo iterations for the mean ISL of CPFSK signals over the sampling cell with respect to the symbol number. The sampling frequency factor is 2.

quency factor α increases, the mean ISL for the proposed filter almost coincides with the one optimized for the on-grid value, for same filter lengths. For sampling frequency rate greater than 2.5, the mean ISL difference between the MMF_0^K and MMF_τ^K is almost insignificant, around 10^{-2} in dB, as shown in Figure 2. We can deduce from the convergence of the two filters that the use of the proposed filter is profitable when the signal is not over-sampled, otherwise the on-grid points are very close to each other and the off-grid problem is negligible, as expected.

Figure 3 displays the mean ISL filter performance for different symbol numbers per CPFSK signal over 50 Monte Carlo iterations. We can remark that the symbol number embedded in the phase is not a constraint factor for the ISL performance, which provides a positive feature in the communications performance. The anticipated result for longer CPFSK signals, which induce larger correlation supports, is an increased ISL over the sampling cell, compared to shorter signals. However, the additional degrees of freedom provided by the larger number of samples seem to allow a better sidelobe reduction by compensating this effect and leading to a global almost invariant ISL with respect to the considered symbol number.

Globally speaking, the best results for the overall average sidelobe energy over the sampling cell are provided by the $3N$-length MMF_τ^{3N} filter.

V. Conclusion

Our paper proposes an optimal mismatched filter which minimizes the average sidelobe energy over a continuous delay interval defined with respect to the sampling cell in order to take into consideration any possible delay shift while using continuous phase frequency-shift keying signals. It introduces a pulse compression technique for a joint radar-communications system, where the need for low sidelobe level energy is essential. The results show that, among several tested filters, the $3N$-length mismatched filter introduced in this paper provides the lowest mean sidelobe energy over the continuous delay interval.

References

[1] N. Levanon *et al.*, *Radar signals*, 3rd ed. IEEE-PRESS, WILEY, 2004.
[2] S. D. Blunt *et al.*, "Overview of radar waveform diversity," *IEEE Aerospace and Electronic Systems Magazine*, 2016.
[3] O. Rabaste *et al.*, "Mismatched filter optimization for radar applications using quadratically constrained quadratic programs," *IEEE Transactions on Aerospace and Electronic Systems*, 2015.
[4] S. D. Blunt *et al.*, "Doppler-compensated adaptive pulse compression," in *IEEE RadarConf*, 2006.
[5] P. Stoica *et al.*, "Transmit codes and receive filters for radar," *IEEE Signal Processing Magazine*, no. 6, 2008.
[6] J. E. Cilliers *et al.*, "Pulse compression sidelobe reduction by minimization of L_p-norms," *IEEE Transactions on Aerospace and Electronic Systems*, 2007.
[7] J. Baden *et al.*, "Optimal peak sidelobe filters for biphase pulse compression," in *IEEE ICR*, 1990.
[8] O. Rabaste *et al.*, "Robust mismatched filter for off-grid target," *IEEE Signal Processing Letters*, 2019.
[9] F. J. Harris, "On the use of windows for harmonic analysis with the discrete fourier transform," *Proceedings of the IEEE*, 1978.
[10] A. De Maio *et al.*, "Design of radar receive filters optimized according to L_p-norm based criteria," *IEEE transactions on signal processing*, 2011.
[11] A. Aubry *et al.*, "Mimo radar beampattern design via PSL/ISL optimization," *IEEE Transactions on Signal Processing*, 2016.
[12] T. Aittomäki *et al.*, "Mismatched filter design for radar waveforms by semidefinite relaxation," in *IEEE ICASSP*, 2015.
[13] O. Rabaste *et al.*, "Off-grid target detection with normalized matched subspace filter," in *IEEE EUSIPCO*, 2016.
[14] M.-E. Chatzitheodoridi *et al.*, "A mismatched filter for integrated sidelobe level minimization over a continuous doppler shift interval," in *IEEE RadarConf*, 2020.
[15] J. B. Anderson *et al.*, *Digital phase modulation.* Springer Science & Business Media, 2013.
[16] S. D. Blunt *et al.*, "Polyphase-Coded FM (PCFM) radar waveforms, part I: implementation," *IEEE Transactions on Aerospace and Electronic Systems*, 2014.
[17] M. Grant *et al.*, "CVX: Matlab Software for Disciplined Convex Programming, version 2.1," http://cvxr.com/cvx, Mar. 2014.
[18] J. G. Proakis, *Digital communications.* McGraw-Hill, 1983.
[19] O. Rabaste *et al.*, "Approximated optimal mismatched filter for off-grid-delayed sampled continuous-phase modulations," in *ICR*, 2017.
[20] X. Lu *et al.*, "Parameter assessment for SAR image quality evaluation system," in *IEEE APSAR*, 2007.